ЖУРНАЛ СТРУКТУРНОЙ ХИМИИ

2015. Том 56, № 7 *Декабрь* *С. 1389 – 1397*

UDC 548.737:541.65

HOST—GUEST ASSOCIATION OF MORIN WITH β-CD AND C-HEXYLPYROGALLOL[4]ARENE: STRUCTURE OF THE COMPLEXES AND THE EFFECT OF pH

S. Chandrasekaran[1], I.V. Muthu[1], V. Enoch[1,2]

[1]*Department of Chemistry, Karunya University, Coimbatore, Tamil Nadu, India*
E-mail: drisraelenoch@gmail.com
[2]*Department of Nanosciences and Technology, Karunya University, Coimbatore, Tamil Nadu, India*

Received March, 19, 2014

The study of the host—guest association of Morin hydrate (MO) with β-cyclodextrin (β-CD) and C-hexylpyrogllol[4]arene (C-HPA) is reported in this paper. The iInclusion complexation of MO is studied by ultraviolet-visible, steady-state fluorescence, time-resolved fluorescence, ^{1}H nuclear magnetic resonance (NMR), and two dimentional rotating-frame nuclear overhauser effect correlation (2D ROESY) spectroscopic techniques. The stoichiometry and the binding constant for the MO—β-CD complex are derived from the linearity of the Benesi—Hildebrand equation. The binding constant for the MO—C-HPA complex is calculated from the nonlinear curve fitting of fluorescence intensities. The effects of the acid strength on the absorption and fluorescence spectra of MO are studied in the absence and the presence of β-CD/C-HPA host molecules. The pK_a values of the ground and the excited states are reported.

DOI: 10.15372/JSC20150713

K e y w o r d s: host—guest complex, morin, β-cyclodextrin, C-hexylpyrogallol[4]arene, fluorescence spectroscopy.

INTRODUCTION

Morin (3,5,7,2′,4′-pentahydroxyflavone) is a flavonol commonly found in old fustic (*Chlorophora tinctoria*), almonds (*P. guajava L.*), mill (*Prunus dulcis*), fig (*Chlorophora tinctoria*), onion, and apple. It possesses various biological activities, including anti-oxidation, anti-mutagenesis, anti-inflammation, anticancer, protein kinase C inhibitor, and cell proliferation inhibitor [1—3]. Morin has been found to influence blood ammonia, plasma urea, and lipid peroxidation in an animal model of AC induced hyperammonemia [4]. Furthermore, morin decreases the oxidative damage of cardiovascular cells [5, 6], lung fibroblast cells [7], and neurons [8]. A morin dose does not show any toxicity in experimental animals even at a high concentration for a prolonged period [9].

Pyrogallol[4]arenes belong to a class of container molecules and molecular capsules obtained by both covalent binding and self-assembly through non-covalent interactions [10, 11]. These molecules can reversibly encapsulate different guest chemical species in the formed self-assembled structures. Of different non-covalent self-assembled molecular capsules prepared and studied over the past decade calixarenes and pyrogallolarenes were studied extensively [12—14]. A particularly intriguing property is their ability to isolate the encapsulated guests from the bulk. These molecular capsules are capable of enantioselective recognition [15], isolation, and catalyzing reactions within their cavities [16].

Cyclodextrins (CDs) are tapered cone shaped cyclic oligosaccharides, mostly consisting of six, seven, and eight glucose units for α-CD, β-CD, and γ-CD respectively. They have relatively non-polar

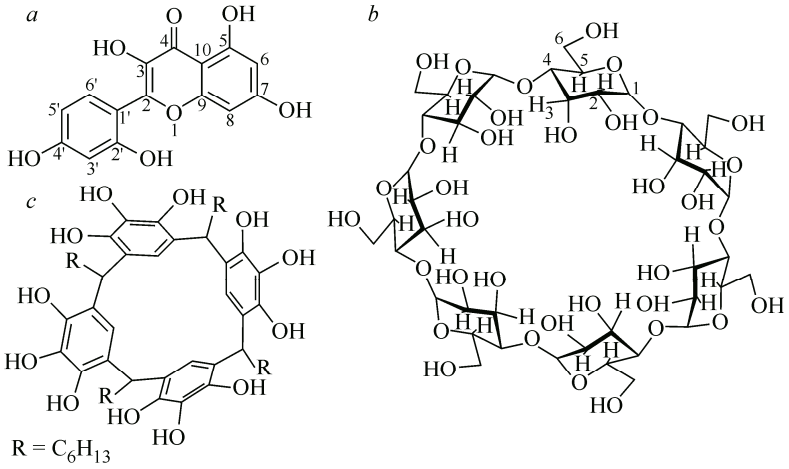

Fig. 1. (*a*) Structure of MO, (*b*) Structure of β-CD, (*c*) Structure of C-HPA

cavities capable of accommodating a variety of guest molecules to form inclusion complexes. Non-covalent intermolecular forces play a key role in the complex formation and its stabilization. This property leads to widespread applications in pharmaceutical chemistry, food technology, analytical chemistry, chemical synthesis, and catalysis [17—20]. A large amount of work has been done to understand the inclusion complexation between cyclodextrins and guest molecules under different conditions. In this paper we report the association of morin (MO) with the two host molecules, *viz*., C-hexylpyrogallol[4]arene (C-HPA) and β-cyclodextrin (β-CD). We have intended to study in detail the stoichiometry, the binding constant, the binding mode, and the structure of morin complexes with host structures and the effect of acidity on the complexes.

EXPERIMENTAL

Chemicals. Morin hydrate and β-cyclodextrin were purchased from Sigma—Aldrich and Hi Media respectively and used as received. Phosphoric acid and sodium hydroxide, used to adjust the pH of the solution, were products of Qualigens. A modified Hammett acidity scale [21] was used for the measurement of H_0 and pH below 2. C-Hexylpyrogallol[4]arene was prepared by the reaction of heptaldehyde and pyrogallol (products of Sigma—Aldrich), following the literature procedure [22]. All the solvents used (Merck) were of spectral grade and were used without further purification.

Preparation of the MO—C-HPA inclusion complex. Equimolar amounts of MO (0.1 g, 3.31×10^{-4} mol) and C-HPA (0.29 g) were separately dissolved in ethanol in 50 ml beakers. A MO solution was added slowly to the C-HPA solution at room temperature in an Ultra-sonicator for 30 minutes. Then the mixture was warmed to 50 °C for 10 minutes and kept at room temperature for a day to crystallize out. The obtained solid was collected, recrystallized, and analyzed.

Preparation of test solutions. Test solutions were prepared by the appropriate dilution from a stock MO solution of 1.0582×10^{-4} mol·dm^{-3}. The stock solution was prepared in ethanol due to the poor solubility of MO in water. The test solutions were having the concentration of 1% ethanol. Stock β-CD solutions at a concentration of 1.2×10^{-2} mol·dm^{-3}, and a stock C-HPA solution of 2×10^{-5} mol·dm^{-3} were used for the preparation of test solutions. Various concentrations of sulfuric acid (0.25 mol·dm^{-3}, 0.5 mol·dm^{-3}, 1.0 mol·dm^{-3}, 2.0 mol·dm^{-3}, 3.0 mol·dm^{-3}, and 4.0 mol·dm^{-3}) were used to vary the acid strength and H_0 values were interpreted from a modified Hammett acidity scale. All the reagents and solvents were of spectral grade and were used without further purification. Doubly distilled water was used throughout the experiments. All experiments were carried out at ambient temperature of 25±2 °C. The test solutions were homogeneous after all additives were added and the absorption and the fluorescence spectra were measured against appropriate blank solutions.

Instrumentation. Absorption measurements were performed on a double beam UV-Visible spectrophotometer (Jasco V-630) using 1 cm path length cells. A spectrofluorimeter (Perkin-Elmer LS55) equipped with a 120 W Xenon lamp for excitation served for the measurement of fluorescence. Both excitation and emission bandwidths were set up at 4 nm. Time-resolved fluorescence measurements were performed on a time-correlated single photon counting HORIBA spectrofluorimeter using a LED source. A PCI 9L 250H ultra-sonicator (India) was used for sonication. pH studies were carried out using an Elico LI 120 pH meter (India). ^{1}H NMR and 2D ROESY spectra were recorded on a Bruker AV III instrument operating at 500 MHz with $CDCl_3$ for MO, C-HPA, and the MO—C-HPA complex.

Table 1

Absorption and fluorescence spectral data of MO *at various* β-CD *concentrations*

β-CD conc., mol·dm^{-3}	Absorption maximum, nm	Absorbance, a.u.	Fluorescence maximum, nm	β-CD conc., mol·dm^{-3}	Absorption maximum, nm	Absorbance, a.u.	Fluorescence maximum, nm
0	390.0	0.1042	507.0	8.0×10^{-3}	389.0	0.1220	504.0
2.0×10^{-3}	390.0	0.1096	506.5	1.0×10^{-2}	389.0	0.1255	503.5
4.0×10^{-3}	390.0	0.1178	506.0	1.2×10^{-2}	389.0	0.1329	502.0
6.0×10^{-3}	389.0	0.1190	505.0				

The chemical shift values are reported in ppm. Tetramethylsilane (TMS) was used as the internal standard. The chemical shift values were obtained downfield from TMS in ppm. The mixing time for ROSEY spectra was 200 ms under the spin lock condition.

RESULTS AND DISCUSSION

Host—guest association of MO with β-CD. The absorption and fluorescence spectral data of MO with various concentrations of β-CD are given in Table 1. The increase in the absorbance of MO with increasing β-CD concentration from 0 to 1.2×10^{-2} mol·dm^{-3} is shown in Fig. 2, *a*. There are two absorption bands of MO, observed at 261 nm and 390 nm, corresponding to $n \rightarrow \pi^*$ and $\pi \rightarrow \pi^*$ transitions respectively. There is a blue shift of 2 nm observed in the absorption bands when β-CD is added. The absorption spectrum with a blue shift shows that there is dislodging of a MO molecule from the polar solvent environment to the hydrophobic nonpolar environment of the β-CD cavity to increase with the β-CD concentration. The fluorescence spectrum of MO with the addition of various amounts of β-CD is shown in Fig. 2, *b*. There are two fluorescence emission bands, *viz*., at 444 nm and 507 nm. The addition of β-CD in an increasing concentration leads to an increase in the fluorescence intensity of MO with the blue shift. This is due to the MO encapsulation in the hydrophobic cavity of a β-CD molecule, which restricts the molecular vibration of MO. Using equation (1), the linearity (with the correlation coefficient $R = 0.99$) is observed in the Benesi—Hildebrand plot for an increase in the

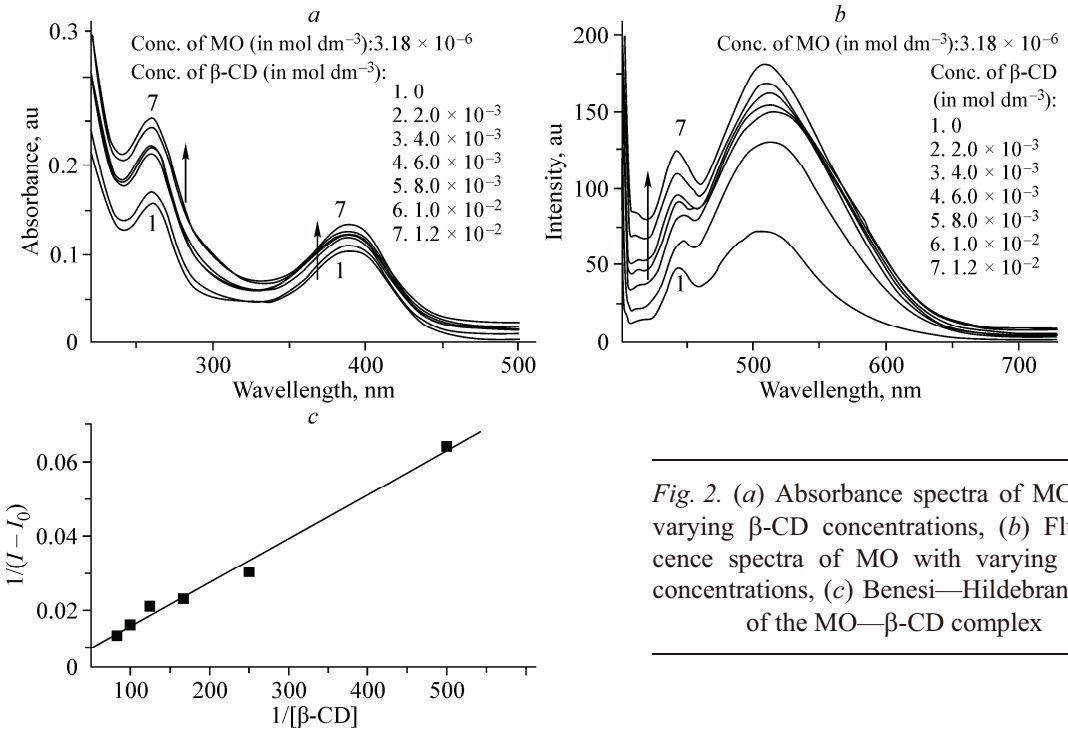

Fig. 2. (*a*) Absorbance spectra of MO with varying β-CD concentrations, (*b*) Fluorescence spectra of MO with varying β-CD concentrations, (*c*) Benesi—Hildebrand plot of the MO—β-CD complex

Table 2

Time-resolved fluorescence spectral data of MO *in water and* β-CD

β-CD conc., mol·dm^{-3}	Lifetime, s	Relative amplitude, %	χ^2	Standard deviation, s	β-CD conc., mol·dm^{-3}	Lifetime, s	Relative amplitude, %	χ^2	Standard deviation, s
0	6.12×10^{-9}	100	1.0580	3.91×10^{-11}	0.012	7.53×10^{-10}	48.44	1.1555	1.09×10^{-11}
0.001	1.66×10^{-9}	76.26	1.1629	1.58×10^{-11}		5.99×10^{-9}	51.56		3.13×10^{-11}
	4.85×10^{-9}	23.74		4.26×10^{-11}					

fluorescence intensity as a function of β-CD. The linear plot of $1/(I - I_0)$ *vs*. 1/[β-CD] is shown in Fig. 2, *c*. Equation (1) is as follows:

$$\frac{1}{I - I_0} = \frac{1}{I' - I_0} + \frac{1}{I' - I_0}\frac{1}{K[\beta\text{-CD}]}, \quad (1)$$

where I_0 is the fluorescence intensity of MO in water, I is the intensity at each concentration of β-CD, and I' is the fluorescence intensity at the highest β-CD concentration. K is the binding constant. The stoichiometry for the formed MO—β-CD complex is determined as the 1:1 ratio and the binding constant K is calculated as 1.11×10^2 mol^{-1}·dm^3.

The complex formation of MO with β-CD is further confirmed by time-resolved fluorescence spectroscopy. The time-resolved spectral data on MO with water and increasing β-CD concentration are given in Table 2. In water, MO shows a mono-exponential decay with the life span of 6.12×10^{-9} s (relative amplitude 100), and it becomes bi-exponential with an increase in the β-CD concentration. MO lifetimes at a high β-CD concentration (1.2×10^{-2} mol·dm^{-3}) are 7.53×10^{-10} s and 5.99×10^{-9} s at a bi-exponential decay with the observed relative amplitudes of 48.44 and 51.56 respectively. The newly formed species gradually increases in the fluorescence lifetime with an increase in the β-CD concentration. The increased lifetime of a newly formed species is stabilized by the host—guest interaction of MO with β-CD. The conversion of the mono-exponential decay into the bi-exponential decay of MO by the addition of β-CD in the time-resolved profile confirms the formation of the 1:1 stoichiometry ratio of the MO—β-CD complex.

Host—guest association of MO with C-HPA. The titration of MO with an increase in the C-HPA concentration from 0 to 2.72×10^{-5} mol·dm^{-3} shows an increase in the absorbance of UV-visible absorption bands and an enhancement of fluorescence, as illustrated in Fig. 3, *a* and *b* respectively. The absorption and fluorescence maxima during the association of MO to the C-HPA host molecule are given in Table 3. The intensities of the absorption and fluorescence spectra of MO in water are hyperchromically shifted on the addition of C-HPA aliquots mainly due to the guest—host interactions. A strong blue shift of 9 nm (390 nm to 371 nm) in the absorption spectrum occurs due to the migration of the MO molecule from the hydrophilic solvent cage in water (0 mol·dm^{-3} of C-HPA) to the π electron rich hydrophobic cavity of the C-HPA molecule. This is due to the host—guest interaction between the C-HPA and MO molecules. The fluorescence intensities at the 507 nm band of MO strongly increase with an increase in the C-HPA concentration. It results in a non-linear curve. The

Table 3

Absorption and fluorescence spectral data of MO *at various* C-HPA *concentrations*

C-HPA conc., mol·dm^{-3}	Absorption maximum, nm	Absorbance, a.u.	Fluorescence maximum, nm	C-HPA conc., mol·dm^{-3}	Absorption maximum, nm	Absorbance, a.u.	Fluorescence maximum, nm
0	390.0	0.1025	507.0	1.52×10^{-5}	384.0	0.1656	507.5
3.18×10^{-6}	**389.0**	**0.1207**	**507.0**	1.92×10^{-5}	383.0	0.1940	508.0
7.18×10^{-6}	388.0	0.1306	507.0	2.32×10^{-5}	382.0	0.2101	508.0
1.12×10^{-5}	387.0	0.1487	507.5	2.72×10^{-5}	381.0	0.2216	508.0

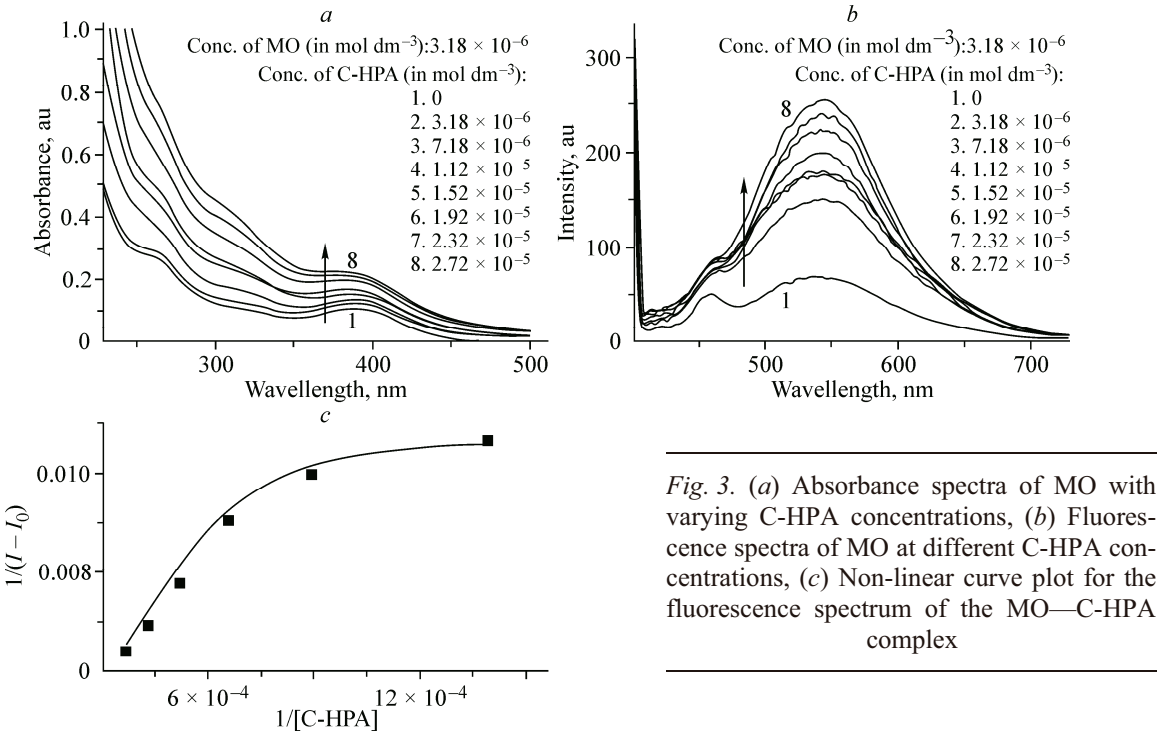

Fig. 3. (*a*) Absorbance spectra of MO with varying C-HPA concentrations, (*b*) Fluorescence spectra of MO at different C-HPA concentrations, (*c*) Non-linear curve plot for the fluorescence spectrum of the MO—C-HPA complex

data were fitted using a non-linear curve fitting for the below equilibrium

$$G + H \rightleftarrows C, \tag{2}$$

where G represents MO (Guest), H represents C-HPA (Host), and C refers to the inclusion complex. The binding constant (K_{11}) for the 1:1 complex is determined as 6.40×10^4 mol^{-1}dm^3 from the fitting of the data in the following equation, [23]:

$$\Delta I = \frac{\Delta I_{11}\left\{\left([G_0]+[H_0]+\frac{1}{K_{11}}\right)-\sqrt{\left([G_0]+[H_0]+\frac{1}{K_{11}}\right)^2-4[G_0][H_0]}\right\}}{2[G_0]}, \tag{3}$$

where G_0 is the initial concentration of the guest, H_0 is the initial concentration of the host, K_{11} is the binding constant of the 1:1 complex, and ΔI_{11} is the intensity difference between the free and complexed forms of the fluorophore. The binding curve for the MO—C-HPA binding is shown in Fig. 3, *c*. This corresponds to a 1:1 stoichiometry of the host—guest complex.

The time-resolved fluorescence measurements of MO in the absence and presence of C-HPA were recorded and the fluorescence lifetime, relative amplitude, χ^2 (refers to the fit of the curve), and the standard deviation data are given in Table 4. The time-resolved decay profile of MO in water (in the absence of C-HPA) is mono-exponential whereas an increase in the C-HPA concentration resulted in the bi-exponential decay. The host–guest interaction of MO and C-HPA results in a new increased lifetime for the MO—C-HPA complex formed. In order to further confirm the host—guest interactions

T a b l e 4

Time-resolved fluorescence spectral data of MO *in water and* C-HPA

C-HPA conc., mol·dm^{-3}	Lifetime, s	Relative amplitude, %	χ^2	Standard deviation, s	C-HPA conc., mol·dm^{-3}	Lifetime, s	Relative amplitude, %	χ^2	Standard deviation, s
0	6.12×10^{-9}	100	1.0580	3.91×10^{-11}	3.0×10^{-5}	8.72×10^{-10}	48.65	1.1925	1.10×10^{-11}
3.0×10^{-6}	1.14×10^{-9}	54.98	1.1137	1.37×10^{-11}		6.10×10^{-9}	51.35		3.16×10^{-11}
	5.81×10^{-9}	45.02		3.19×10^{-11}					

Table 5

^{1}H NMR *spectral data of* MO, C-HPA, *and the* MO—C-HPA *complex*

C-HPA		MO			MO—C-HPA complex
Nature of protons	Chemical shift, δ (ppm)	Nature of protons and position	Chemical shift, δ (ppm)	Nature of peaks	Chemical shift, δ (ppm)
C-hexyl chain		Aromatic protons			
Methyl protons	0.93	H-6	6.17	Doublet	5.96
Methylene protons	1.28—1.45	H-8	6.29	Doublet	6.06
CH — linked in pyrogallol rings	2.21—2.28	H-5′	6.34—6.36	Doublet of doublet	6.10—6.12
		H-3′	6.39	Doublet	6.23
		H-6′	7.22—7.24	Doublet	7.01—7.03
Pyrogallol unit		Hydroxyl groups			
Aromatic protons	7.49	OH-3	8.03—8.05	Doublet of doublet	7.79—7.82
Hydroxyl protons	6.86, 6.90 and 8.80	OH-4′	9.39	Singlet	8.37
		OH-7	9.77	Singlet	8.41
		OH-2′	10.71	Singlet	10.32
		OH-5	12.62	Singlet	11.48
		H_2O	3.39	Singlet	3.27

between MO and C-HPA, ^{1}H NMR and 2D ROESY spectroscopic techniques were used, which are discussed in the next section.

NMR analysis. The ^{1}H NMR chemical shift values of C-HPA, MO, and the MO—C-HPA complex are summarized in Table 5. The MO complexation with the C-HPA host leads to an up-field shift of ^{1}H NMR signals for the MO—C-HPA complex compared to the signals of the MO molecule. Intermolecular proton interactions of MO with C-HPA were observed in the 2D ROESY NMR spectrum. A cross peak is observed which corresponds to the interaction of the MO hydroxyl proton at position 3 with the C-HPA hydroxyl protons (marked with a circle in Fig. 4). This peak appears due to the cross correlation of a flavanone moiety of the MO guest molecule to the pyrogallol units of the

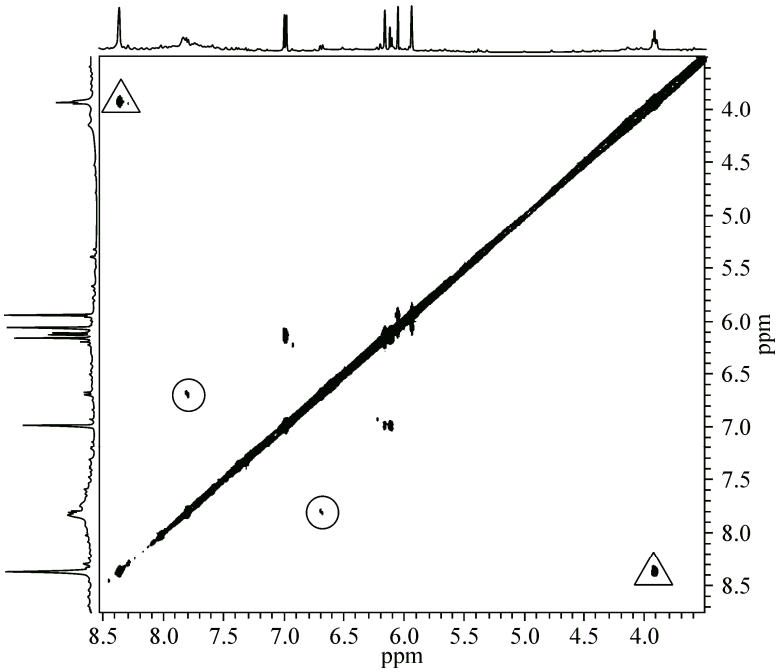

Fig. 4. 2D ROESY NMR spectrum of the MO—C-HPA complex

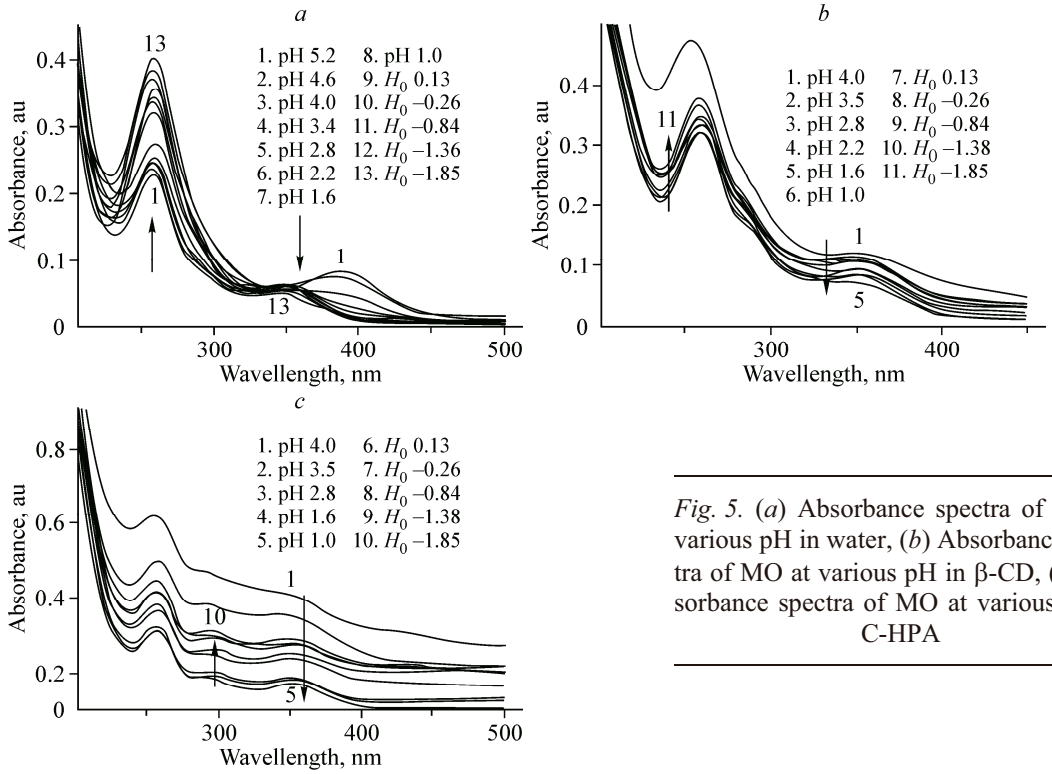

Fig. 5. (*a*) Absorbance spectra of MO at various pH in water, (*b*) Absorbance spectra of MO at various pH in β-CD, (*c*) Absorbance spectra of MO at various pH in C-HPA

host C-HPA molecule. Another off-diagonal peak (marked with a triangle) is observed due to the correlation of the MO hydroxyl proton at position 7 with the aromatic C—H proton of pyrogallol rings in the C-HPA molecule. This correlation peak arises due to the close proximity of guest and host molecules by the insertion of MO molecules into the π electron clouds of the C-HPA aromatic rings. Thus, the host—guest interactions of MO with C-HPA are supported by the 2D ROESY NMR spectrum.

Effect of acid on MO. Fig. 5, *a* shows the effect of pH on the absorption spectrum of MO in water. A large blue shift of MO absorbance decreases from the pH of 5.2 to H_0 –1.85. The blue shift of the absorption band from 388 nm decreases in absorbance and the increased intensity of the 258 nm bands was observed due to the formation of a MO monocation on acidification. This occurs at an increased proton concentration in the solution. There is an isosbestic point at around 333 nm due to the equilibrium between the neutral and protonated forms of MO at a given pH. The ground state pK_a value can be obtained for this equilibrium from equation (4)

$$C_1 = \frac{A(\lambda_1)\varepsilon_2(\lambda_2) - A(\lambda_2)\varepsilon_2(\lambda_1)}{\varepsilon_2(\lambda_1)\varepsilon_2(\lambda_2) - \varepsilon_1(\lambda_2)\varepsilon_2(\lambda_1)}, \quad (4)$$

$$C_2 = C_T - C_1, \quad (5)$$

where C_T is the total concentration of the compound in both forms and $\varepsilon_1(\lambda_1)$, $\varepsilon_2(\lambda_2)$, $\varepsilon_2(\lambda_1)$, $\varepsilon_2(\lambda_2)$ are the molar extinction coefficients of the protonated and neutral forms at wavelengths λ_1 and λ_2 respectively (258 nm and 388 nm in this case). The pK_a for the equilibrium of the protonated—neutral forms is calculated using equation (6). The calculated ground state pK_a of the neutral—monocation equilibrium of MO in water is –0.42±0.03.

$$pK_a = pH + \log C_1 / C_2. \quad (6)$$

The effect of acid on the absorption spectrum of MO in β-CD is shown in Fig. 5, *b*. In the presence of β-CD, the added acid concentration of a MO molecule shows a blue shift of the absorption band down from pH 4.0 to H_0 –1.85. The two absorption bands observed at 258 nm and 353 nm decrease (the band at 353 nm) up to pH 1.6 and gradually increase (the band at 258 nm). The absorption band at 258 nm increases continually from pH of 1.0 up to H_0 –1.85 and the enhanced band merges with the band in the pH range from 4.0 to 1.6. Hence, the isosbestic point of the formation of the

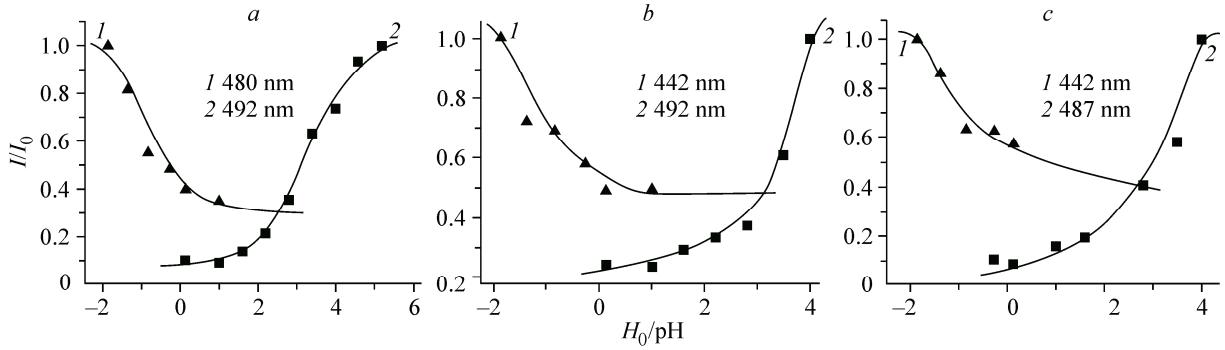

Fig. 6. (*a*) I/I_0 plot versus H_0/pH plot of MO in water, (*b*) I/I_0 plot versus H_0/pH plot of MO in β-CD, (*c*) I/I_0 plot versus H_0/pH plot of MO in C-HPA

monocationic equilibrium could not be found exactly. The blue shift is observed in the absorption spectrum on acidification due to the increased proton concentration on a MO molecule. There is a small blue shift observed, which may be due to the presence of β-CD that to a certain extent shields the MO molecule from protonation by the inclusion complexation. The similar result was observed for the effect of acid on the absorption spectra of MO with C-HPA (Fig. 5, *c*).

The fluorescence intensity decreases at 492 nm at pH of 5.2 and increases in the band at 442 nm after pH is 1.0 moving to H_0 –1.85. A shift of the fluorescence band towards blue with the formation of a new band shows the neutral—monocation MO formation with an increase in the proton concentration. From the fluorescence intensities at the two maxima the sigmoidal intercept curve for the neutral—monocation equilibrium is obtained. This plot resulted in the excited state pK_a (pK_a*) of –0.47± ±0.02. The intercept plot between H_0/pH *vs.* I/I_0 is shown in Fig. 6, *a*.

The fluorescence emission spectrum of MO in the presence of β-CD shows the quenching when the acid is added up to pH 1.0 and an increase in the intensity on acidification to H_0 –1.85. This change in the fluorescence intensity with the shift of the blue region is due to the existence of the equilibrium within the neutral—monocationic MO system with β-CD. The plot of relative intensities (442 nm and 492 nm) with various H_0/pH were drawn and pK_a* is obtained from the monocation formation curve as –0.93±0.02. This pK_a* value is almost 2 times higher in the acid concentration as compared to pK_a* obtained from the effect of the acid strength on MO in water. The high pK_a* value resulted from the inclusion of MO to the cavity of β-CD molecules which acted as a shield from the protonation of MO. The change in the fluorescence spectrum of the MO in the presence of β-CD caused by acidification resulted in the I/I_0 *vs*. H_0/pH plot at the two maxima (492 nm and 442 nm) is shown in Fig. 6, *b*.

The changes in the acid strength in the MO solution in the presence of C-HPA were also studied. Upon acidifying MO in the presence of C-HPA, the fluorescence intensity decreases at 487 nm up to H_0 0.13 and increases at 442 nm up to H_0 –1.85 and the fluorescence maxima of MO in C-HPA is blue-shifted. The pK_a* value of –0.95±0.02 is obtained from the neutral-monocation formation equilibrium curve and is shown in Fig. 6, *c*. The pK_a* value is twice higher than the pK_a* value obtained for MO in water and nearly equal in the presence of the β-CD solution. Higher pK_a* values shown for the MO molecule might be protected by the C-HPA host molecules. Hence, from the obtained results it can be concluded that the MO molecule can be involved in the host—guest interactions with the β-CD/C-HPA host molecules. Based on the above results, the structural representation for the guest—host interactions of MO with the β-CD/C-HPA host molecules are shown in Fig. 7.

CONCLUSIONS

Host—guest interactions of the MO molecule are studied with the host systems such as β-CD and C-HPA by UV-visible, steady-state fluorescence, time-resolved fluorescence, and 2D ROESY NMR spectroscopic techniques. The 1:1 stoichiometry was inferred from the Benesi—Hildebrand equation for the MO—β-CD complex and the binding constant K is 1.11×10^2 mol^{-1}dm^3. For the fluorescence

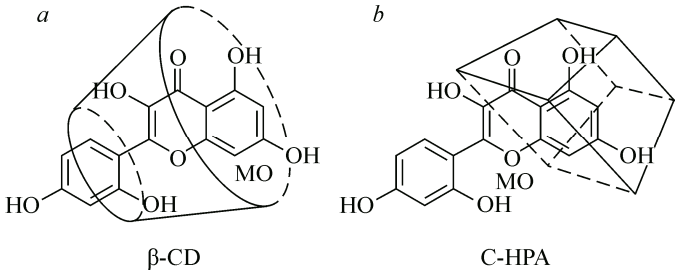

Fig. 7. Schematic interaction of MO with β-CD and C-HPA

intensities of the MO—C-HPA complex, the non-linear curve fitting was employed and the binding constant (K_{11}) value is 6.40×10^4 $mol^{-1}dm^3$ and the stoichiometry is 1:1. The complex formation is further evidenced by the increased lifetimes of the states and the relative amplitude of MO in the presence of β-CD/C-HPA host molecules in the time-resolved fluorescence profile. 2D ROESY NMR spectra also support the formation of the MO—C-HPA complex by showing cross peaks between the MO and C-HPA protons. In addition, the host—guest interactions of MO with β-CD/C-HPA molecules are studied with regard to the effect of the acid strength. The ground and the excited state pK_a values of MO in water and in β-CD or in C-HPA are reported. The change in the pK_a values of MO in the absence and presence of host molecules supports the formation of the host—guest complex.

This work is financially supported by the Department of Science and Technology (DST), Government of India (Project file: SR/FT/CS-062/2009). We express our gratitude to DST. We thank SAIF, Indian Institute of Technology—Madras, Chennai, for their help in NMR measurements. We extend our thanks to the Dean—Research, the Registrar, the Vice—Chancellor, and the Chancellor of Karunya University for providing the necessary facilities.

REFERENCES

1. *Sivaramakrishnan V., Moorthy Shilpa P.N., Praveen Kumar V.R. et al.* // Chem.-Biol. Interact. – 2008. – **171**. – P. 79 – 88.
2. *Rui Zhang R., Kang A.K., Jing Piao M. et. al.* // Chem.-Biol. Interact. – 2009. – **177**. – P. 21 – 27.
3. *Sivaramakrishnan V., Niranjali Devaraj S.* // Chem.-Biol. Interact. – 2010. – **183**. – P. 284 – 292.
4. *Subash S., Subramanian P.* // Asian Pac. J. Trop. Dis. – 2012. – P. 103 – 106.
5. *Wu T.W., Zeng L.H., Wu J. et al.* // Biochem. Pharmacol. – 1994. – **47**. – P. 1099 – 1103.
6. *Kok L.D., Wong Y.P., Wu T.W. et al.* // Life Sci. – 2000. – **67**. – P. 91 – 99.
7. *Zhang R., Kang K.A., Piao M.J. et al.* // Chem.-Biol. Interact. – 2009. – **177**. – P. 21 – 27.
8. *Ibarretxe G., Sanchez-Gomez M.V., Campos Esparza M.R. et al.* // GLIA. – 2006. – **53**. – P. 201 – 211.
9. *Yugarani T., Tan B.K., Teh M. et al.* // Lipids. – 1992. – **27**. – P. 181 – 186.
10. *Cram D.J.* // Nature. – 1992. – **356**. – P. 29 – 36.
11. *Conn M.M., Rebek J. Jr.* // Chem. Rev. – 1997. – **97**. – P. 1647 – 1668.
12. *Hamann B.C., Shimizu K.D., Rebek J. Jr.* // Angew. Chem. Int. Ed. Engl. – 1996. – **35**. – P. 1326 – 1329.
13. *Shivanyuk A., Friese J.C., Doring S. et al.* // J. Org. Chem. – 2003. – **68**. – P. 6489 – 6496.
14. *Rebek J. Jr.* // Chem. Commun. – 2000. – P. 637 – 643.
15. *Prins L.J., Verhage J.J., de Jong F. et al.* // Chem.-Eur. J. – 2002. – **8**. – P. 2302 – 2313.
16. *Ito H., Kusukawa T., Fujita M.* // Chem. Lett. – 2000. – 598 – 599.
17. *Szejtli J.* Cyclodextrin and Their Inclusion Complexes. – Budapest: Akademiai Kiado, 1982.
18. *Li S., Purdy W.C.* // Chem. Rev. – 1992. – **92**. – P. 1457.
19. *Szejtli J.* In: Cyclodextrin Technology. – Dordrecht: Kluwer Academic Publishers, 1988.
20. *Wenz G.* // Angew. Chem. Int. Ed. Engl. – 1994. – **33**. – P. 803.
21. *Jorgenson M., Hartter D.R.* // J. Am. Chem. Soc. – 1963. – **85**. – P. 878.
22. *Cave G.W.V., Antesberger J., Barbour L.J. et al.* // Angew. Chem. Int. Ed. – 2004. – **43**. – P. 5263 – 5266.
23. *Douhal A.* Cyclodextrin Materials Photochemistry, Photophysics and Photobiology. – Amsterdam: Elsevier, 2006. – **1**. – P. 9 – 11.